Action potential solitons and waves in axons

Gaspar Cano¹ and Rui Dilão^{2,3}

August 6, 2019 DRAFT 12

1-European Space Agency, ESTEC, Keplerlaan 1, 2201AZ Noordwijk,
Netherlands
2-University of Lisbon, Instituto Superior Técnico, Av. Rovisco Pais, 1049-001
Lisbon, Portugal
3-Institut des Hautes Études Scientifiques, 35, route de Chartres, 91440
Bures-sur-Yvette, France

ruidilao@tecnico.ulisboa.pt gaspar.fcano@gmail.com

Abstract

We show that the action potential signals generated inside axons propagate as reaction-diffusion solitons or as reaction-diffusion waves, refuting the Hodgkin and Huxley (HH) hypothesis that action potentials propagate along axons with an elastic wave mechanism. Action potential signals are solitary propagating spikes along the axon, occurring in a type I intermittency regime of the HH model. Reaction-diffusion action potential wave fronts annihilate at collision and at the boundaries of axons with zero flux, in contrast with elastic waves, where amplitudes add up and reflect at boundaries. We calculate numerically the values of the speed of the action potential spikes, as well as the dispersion relations. These findings suggest several experiments as validating and falsifying tests for the HH model.

Keywords: Action potential waves, Hodgkin-Huxley model, reaction-diffusion waves, reaction-diffusion solitons.

1 Introduction

The electrophysiological states of cells and axons are characterised by an electric potential drop across the cellular membrane, which is maintained through the exchange of ions between the cytoplasm and the intercellular space, [17], [18], and [19]. To describe the electrical properties of axonal signalling, in a sequence of papers, Hodgkin and Huxley (HH) introduced a mathematical model aiming to describe the propagation of action potentials in the axoplasm and which they have compared with voltage clamp data taken from the axon of the squid *Loligo*, [9].

In current clamp experiments, one of the electrodes is located in the extracellular space and the second one is a thin wire introduced longitudinally into the axon, [22], [14, p. 143]. When the axon is electrically excited away from inner electrode, the measured electrical potential drop is a spiky (negative) signal that evolves in time, [10, p. 24]. In principle, this signal results from a longitudinally propagating signal — the action potential — measured by the inner electrode inside the axon.

The derivation of the HH mathematical model for the action potential phenomenon is based on the analogy between the potential difference measured on both sides of the cellular membrane and an electric circuit containing a variable resistance and a power source in series, both in parallel with a capacitor. This analogy is phenomenological, aiming to explain the gating mechanism of ion channels across a cellular membrane through a variable resistance. The power source and the capacitor describe, respectively, a source of energy and a potential energy storage reservoir. The biological functions of the three electric components are unspecified, [22, p. 152], [14, p. 152].

In a synthetic form, the HH model equations are

$$\begin{cases}
\tilde{D}\frac{\partial^{2}V}{\partial x^{2}} = C\frac{\partial V}{\partial t} + F(V, \vec{n}) + i(x, t) \\
\frac{\partial \vec{n}}{\partial t} = \vec{G}(V, \vec{n}),
\end{cases} (1)$$

where t is time, x is the position coordinate along the axon, V(x,t) is the potential drop across the cellular membrane, \tilde{D} is a diffusion coefficient of the potential drop along the axoplasm, C is the phenomenological capacitance of the cellular membrane, and i is a current eventually describing an external forcing, as in current clamp experiments, or simply a neuronal signal originated in the main body of a neurone. The vector function $\vec{n}(x,t) = (n,m,h)$ contains gating variables, specific to ion types. The functions $F(V,\vec{n}): \mathbb{R}^4 \to \mathbb{R}$ and $\vec{G}(V,\vec{n}): \mathbb{R}^4 \to \mathbb{R}^3$ describe, respectively, the local response to the potential drop changes across the cellular membrane and the gating mechanisms of ion channels, [20], [12], [8], [13] and [11].

In [9, p. 522], Hodgkin and Huxley conjecture that the propagation properties of the action potential must be analogous to those of a propagating elastic wave. In fact, they assume the existence of an unknown mechanism which would impose an elastic wave type propagation mechanism inside the axon, such that the transmembrane potential would propagate according to the wave equation

$$\frac{\partial^2 V}{\partial x^2} = \frac{1}{\theta^2} \frac{\partial^2 V}{\partial t^2},\tag{2}$$

where θ is an unknown *ad hoc* longitudinal propagation speed constant. Despite the fact that the solutions of equations (1) and (2) are generically incompatible (equation (1) is of parabolic type and equation (2) is of hyperbolic type), they have substituted the first term of (2) by the first term of (1), obtaining

$$\begin{cases}
\frac{1}{\theta^2} \frac{d^2 V}{dt^2} = \frac{C}{\tilde{D}} \frac{dV}{dt} + \frac{1}{\tilde{D}} F(V, \vec{n}) + \frac{1}{\tilde{D}} i(x, t) \\
\frac{d\vec{n}}{dt} = \vec{G}(V, \vec{n}),
\end{cases} (3)$$

which is an ordinary differential equation. Hodgkin and Huxley integrated numerically the ordinary differential equation (3), for guessed choices of the free parameter θ , and compared them with voltage clamp data. Even though they were able to obtain numerical results similar to their experimental data for some values of the chosen parameters, it should be clear that an ordinary differential equation cannot fully describe a time dependent spatial phenomenon such as the propagation of an electric signal along the axon.

Besides the mathematical inconsistency just described, from the physical and biological points of view, there is a lack of the specific biochemical mechanisms that lead to the electric analog of the model, as evidenced by experimental data, [14]. Several authors, based on physical and chemical principles, provided plausible evidence of the inadequacy of the HH model, [3], [5], [16] and [15].

These simple remarks show that model equations (1) can eventually describe action potential propagation. However, the argument used for its calibration based on equations (3) should be reformulated.

The diffusion free HH model ($\tilde{D}=0$ in (1)) has been extensively analysed from the point of view of its bifurcations, [20], [12], [8] and [4]. This approach has been used as a starting point to obtain simplified models, where parameters lose some of their biological meaning. These simplified models cannot produce predictions about the spatial propagation of action potentials, nor can the existence of Hopf bifurcations predict the generation of action potential signals. In fact, it has been shown in [4] that action potentials are originated by a type I intermittency phenomenon associated with a saddle-node homoclinic bifurcation of limit cycles, which does not exist near Hopf bifurcations.

Some propagation properties of action potential signals have been studied in [1]. These authors have analysed localised high amplitude perturbations of the transmembrane potential of the HH equation and, by manipulating the initial distribution of the membrane potential along the axon, found that action potential fronts propagate as solitary waves, identifying the collisional annihilation of action potential solitary spikes. This has been analysed for several values of the potassium Nernst potential V_K^N , with i=0. These findings are important for the understanding of the fluctuation dynamics of the transmembrane potential, but difficult to observe in axons with voltage clamp experimental techniques. In the present paper, we show that solitary or spiky perturbations only appear in the intermittent regime of the diffusion free equation (1).

More recently, due to the solitary characteristics of action potential signals observed by Hodgkin and Huxley, several authors attempted to explain the solitonic properties of the action potential as a non-linear elastic wave similar to the Korteweg-de Vries equation (eq 9.14 in [2]). This approach is independent from the HH ionic mechanism and has no connection with biological parameters. On the other hand, solitary (elastic) waves of Korteweg-de Vries type are characterised by very precise mechanisms of interaction, with specific rules for amplitude behaviour at interaction and at spatial boundaries, [23]. As we will show below, the waves generated by the HH model equations are reaction-diffusion waves, with different laws of interaction. These different interaction characteristics also appear in chemical kinetics models with reaction-diffusion waves, [21] and [6].

The goal of this paper is to characterise reaction-diffusion waves, reaction-diffusion solitary waves, and reaction-diffusion solitary wave packets in the HH model. Moreover, the analysis of the properties of the HH model and the comparison with experimental data provide a test of the validity and falsifiability of the model.

The paper is organised as follows. In section 2, we review some of the results of the HH partial differential equation model (1), and some of the properties of its solutions, [4]. We also define the parameter settings of the model and summarise the numerical setting of simulations. In section 3, we show numerically that the HH model equations (1) have in fact solitonic and oscillatory solutions, behaving as solitary waves or as solitary wave packets in the intermittent dynamical regime of the diffusion free equation (1), or as oscillatory solutions of the reaction-diffusion equations (1). These results emerge simply as solutions of the equations and it is not necessary to introduce additional mechanisms to explain their propagation inside the axon. We derive the interaction properties of this type of reaction-diffusion waves, and calculate wave speeds and dispersion relations of asymptotic regimes. Finally, in section 4, we propose several experiments for the validation of the HH model and we summarise the main conclusions of the paper.

2 Action potentials propagate as reaction-diffusion waves

In [4], we have exhaustively analysed the solutions of the HH partial differential equations (1), in a spatial one-dimensional domain I = [0, L], with $L < \infty$, and with zero flux boundary conditions. We have chosen the current function: $i(x,t) = i_0$, for x = 0 and every $t \ge 0$, and i(x,t) = 0, otherwise, and we have done the bifurcation analysis of the solutions of the reaction-diffusion equation (1), as a function of the diffusion coefficient \tilde{D} and of the parameter i_0 . This particular choice of the external function i(x,t) simulates current clamp experiments and, for the calibrated parameters, propagating action potentials and action potential wave packets are generated near the left boundary of an axon. Some major conclusions derived from the HH model are important to recall:

- 1) For different choices of the parameters i_0 and $\tilde{D} > 0$, we have found propagating action potential spikes. For positive but small values of i_0 , the shape of the action potentials is caused by a type I intermittent response of the HH equations associated to a saddle-node bifurcation of limit cycles of the diffusion free system of equations ($\tilde{D} = 0$). This particular response is caused by a transient process which anticipates a transition from a dynamics with a unique stable steady state to a dynamics with two limit cycles, one stable and the other unstable. These isolated spikes propagate without attenuation and therefore can be called solitary fronts, solitary waves or solitons. Near the bifurcation, it is possible to obtain single action potential spikes or packets of propagating action potential spikes, depending on the intensity of the perturbation i_0 .
- 2) For larger values of i_0 when compared with case 1), and $\tilde{D} > 0$, we have found propagating periodic waves of action potentials spikes. We have measured numerically the propagation speeds, which depend on the parameters of the model. This propagation speed is not an external parameter, as assumed in equation (2).
- 3) For larger values of i_0 when compared with case 2), and $\tilde{D} > 0$, we have found solutions behaving chaotically and solutions with a long chaotic transient, which, as time passes, converge to a steady homogeneous state (chaotic intermittency) dynamic summary in figure 1.
- 4) The action potential propagation phenomenon only occurs if the current stimulus i_0 at the x = 0 boundary of the axon is large enough and persists for long enough time for the action potential do be fully formed at the current injection point. Once this happens, even if i_0 is set to zero during the spatial

propagation, the action potential will reach the right boundary of the axon without suffering any attenuation.

All these properties of the HH partial differential equation model (1) are predictions about the dynamics of action potentials and should be used to validate the HH model.

To test the above mentioned dynamic features of the HH model, we use the following parameterisation of equation (1)

$$C\frac{\partial V}{\partial t} = \tilde{D}\frac{\partial^{2}V}{\partial x^{2}} - g_{Na}m^{3}h(V - V_{Na}^{N}) -g_{K}n^{4}(V - V_{K}^{N}) - g_{L}(V - V_{L}^{N}) - i$$

$$\frac{\partial n}{\partial t} = \alpha_{n}(V)(1 - n) - \beta_{n}(V)n = G_{n}(V, n)$$

$$\frac{\partial m}{\partial t} = \alpha_{m}(V)(1 - m) - \beta_{m}(V)m = G_{m}(V, m)$$

$$\frac{\partial h}{\partial t} = \alpha_{h}(V)(1 - h) - \beta_{h}(V)h = G_{h}(V, h),$$

$$(4)$$

where

$$\alpha_{n} = 0.01 \phi \frac{V + 10}{e^{(V+10)/10} - 1}, \quad \beta_{n} = 0.125 \phi e^{V/80},
\alpha_{m} = 0.1 \phi \frac{V + 25}{e^{(V+25)/10} - 1}, \quad \beta_{m} = 4 \phi e^{V/18},
\alpha_{h} = 0.07 \phi e^{V/20}, \quad \beta_{h} = \phi \frac{1}{e^{(V+30)/10} + 1},
\phi = 3^{(T-6.3)/10}.$$
(5)

In this equations, V is the transmembrane potential drop measured in mV, i is a transmembrane current density injected into the axon, measured in μ A/cm², and time is measured in ms. Positive values of i correspond to currents flowing from outside to inside the axon. In equation (4), the membrane potential is defined in accordance with the original HH paper, [9], where the action potential voltage spikes are negative. The gating variables n, m and h describe the opening and closing of the channel gates, are specific to the ion type and are dimensionless. The ionic conductances across the cellular membrane are g_{Na} and g_{K} , and g_{L} is a constant measuring "leak" conductance. C is the membrane capacitance and \tilde{D} is a constant inversely proportional to the resistance (Ω), measured along the axon of nerve cells.

The model equations (4)-(5) have been calibrated for the squid giant axon at the temperature T=6.3 °C, [9], and the values of the parameters are: $C=1~\mu\text{F/cm}^2$, $g_{\text{Na}}=120~\text{mS/cm}^2$, $g_{\text{K}}=36~\text{mS/cm}^2$ and $g_{\text{L}}=0.3~\text{mS/cm}^2$, where

S= Ω^{-1} (siemens) is the unit of conductance. The Nernst equilibrium potentials, relating the difference in the concentrations of ions between the inside and the outside of cells with the transmembrane potential drop, are $V_{\rm Na}^N=-115$ mV, $V_{\rm K}^N=12$ mV and $V_{\rm L}^N=-10.613$ mV. This choice of parameters is rescaled in such a way that at rest (i=0), the steady state of the transmembrane potential is $V^*(0)=0$ mV. Hodgkin and Huxley have shown that the transmembrane diffusion coefficient is $\tilde{D}=a/(2R_2)$, where a is the radius of the axon (considered as a cylinder) and R_2 is the specific resistivity along the interior of the axon. For the case of the squid giant axon, $a=238~\mu{\rm m}$, $R_2=35.4~\Omega$ cm and $\tilde{D}=3.4\times10^{-4}~{\rm S}$.

To validate the Hodgkin-Huxley model predictions, we simulate the solutions of the reaction-diffusion equation (4) in a domain of length L=100 cm, with zero flux boundary conditions. The spatial region has been divided into M=800 small intervals of length Δx , where $L=M\Delta x$. We have used an explicit numerical method minimising the global error of the solution, [7]. Let D be the diffusion coefficient, given by $D=\tilde{D}/C$. With the minimising condition $D=\Delta x^2/(6\Delta t)=L^2/(6M^2\Delta t)$, and the choice $\Delta t=0.00765931$ ms, we obtain the diffusion coefficient D=0.34 cm²/ms, or $\tilde{D}=3.4\times 10^{-4}$ S, in agreement with the value suggested by Hodgkin and Huxley, [9].

3 Results

3.1 Overall behaviour of the HH equations

If an axon is initially at rest (V = 0, for all x), it can be perturbed through the transmembrane current $i(x,t) = i_0$, for x = 0 and every $t \ge 0$, and i(x,t) = 0, otherwise. In figure 1, we show how these regions of behaviour depend on the value of i_0 for the chosen diffusion coefficient.

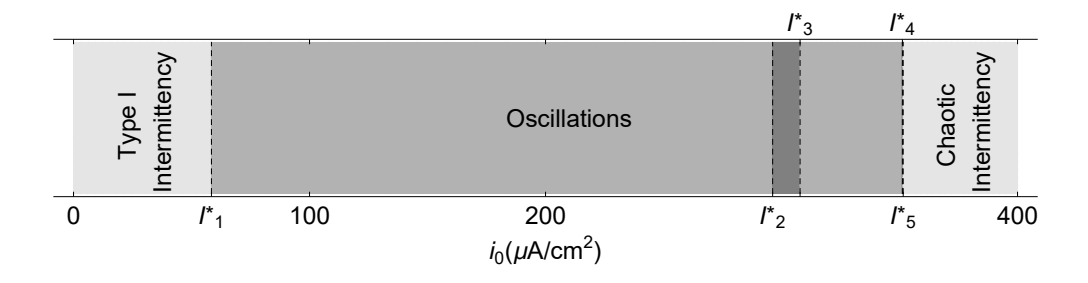


Figure 1: Bifurcation diagram of the solutions of the HH equations (4)-(5), for $\tilde{D} = 3.4 \times 10^{-4}$ S, as a function of the parameter i_0 . For this parameterisation, $I_1^* = 58.44$, $I_2^* = 296.23$, $I_3^* = 307.85$, $I_4^* = 351.21$ and $I_5^* = 351.55$.

For $i_0 < I_1^*$, the system responds with type I intermittency, generating a finite number of action potentials that propagate along the axon before returning to rest. For $i_0 \in [I_1^*, I_5^*]$, the system oscillates indefinitely, never returning to rest. For $i_0 \in [I_1^*, I_2^*] \cup [I_3^*, I_4^*]$, the oscillations asymptotically in time converge to a periodic solution. For the small regions $[I_2^*, I_3^*]$ and $[I_4^*, I_5^*]$, the oscillations show chaotic behaviour with period bifurcations. For $i_0 > I_5^*$, the system shows chaotic intermittency, [4], generating a finite number of action potentials before returning to rest.

3.2 Action potential solitary waves

Since in the HH model the action potentials propagate without attenuation, we can define the characteristic curve of the action potential by the condition dV=0. As $dV=\frac{\partial V}{\partial x}dx+\frac{\partial V}{\partial t}dt=0$, then $\frac{dx}{dt}=-(\frac{\partial V}{\partial t})/(\frac{\partial V}{\partial x})$, implying that action potentials may have a well defined speed. Taking the maxima of the functions -V(x,t) as a reference point, we can follow their space-time evolution. We shall call the curves defined by this condition dV=0 the characteristic curves of the solution of the HH equations (1).

In figure 2, we show the solution of the HH system of equations (4)-(5), responding to an injected current in the type I intermittency parametric region seen in figure 1. In this case, a single action potential spike is generated at the injection point, propagating along the axon and disappearing at the boundary x = L. The characteristic curve of the solutions of the HH equations has a linear profile, which means the action potential propagates along the axon with a constant speed. The slope of the characteristic curve corresponding to the peak of the action potential signal translates to a propagation speed v = 12.14 m/s.

In figure 3, we show the solution of the HH system of equations (4)-(5), again in the region of type I intermittency, generating a total of three action potential sequential signals — packet of spikes. This figure has been obtained for a larger value of i_0 , when compared with the simulations in figure 2. The speed of the first action potential is the same as in figure 2. Even though the characteristic curves corresponding to the second and third spikes appear to also have a linear profile, we will later show that that is not the case, so we refrain from calculating their slope here.

In both figures 2 and 3, the action potentials all propagate without attenuation in their amplitudes and annihilate at the boundary of the axonal domain, never being reflected. This effect cannot be observed with elastic waves. These action potentials behave as solitary reaction-diffusion waves. After the annihilation of the action potentials at the boundary, the axon stays in a non uniform and non excitable state ($i_0 \neq 0$). For a signal to propagate in the axon it is necessary that the electric state of the axon returns to the rest state V = 0 and i = 0, and that the

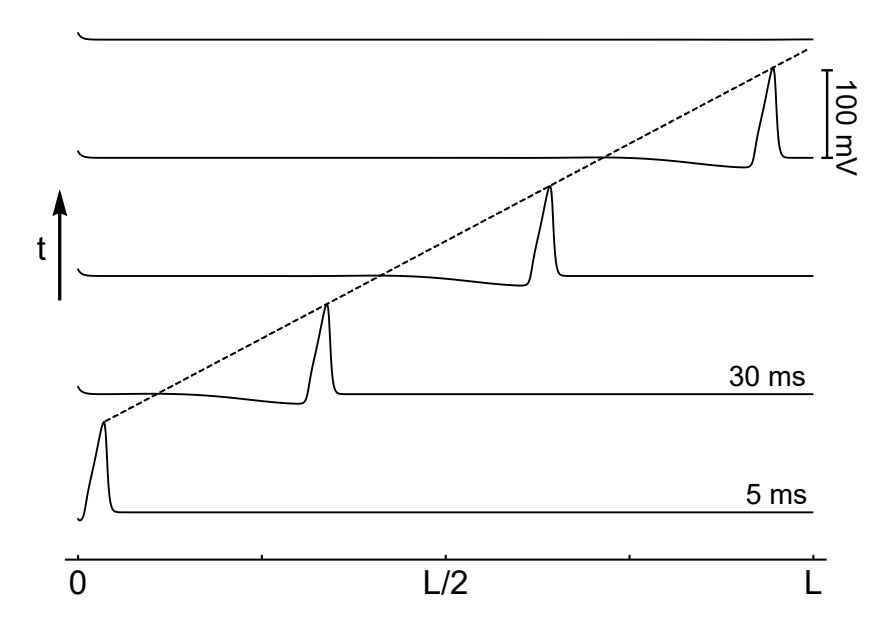


Figure 2: We show five time snapshots of the solutions -V(x,t) of reaction-diffusion equations (4)-(5). The bottom snapshot was taken at t=5 ms, and the succeeding snapshots differ by time intervals $\Delta t=25$ ms. We have considered that the axon is initially at the zero state V(x>0,t<0)=0 and the injected current at x=0 has the value $i_0=55.0~\mu\text{A/cm}^2$, during the entire simulation. The system is in the type I intermittency region (figure 1), generating one spike. The dotted line shows a characteristic curve of the solutions of the HH equations. The propagation speed of the action potential is v=12.14 m/s. The action potential spike annihilates at the boundary x=L, where no reflection occurs.

neurone is again excited with a current above threshold.

In figure 4, we analyse the case where two current sources are injected in the interior of the axon, at the longitudinal coordinates x = L/3 and x = 2L/3. At each injection point, one action potential spike response is generated, and then each of them splits into two action potential spikes, propagating in opposite directions. These four action potentials have the same amplitude as the action potentials in figures 2 and 3. Then, at a later time, the two action potentials that travel towards the center of the axon collide at x = L/2, and annihilate each other — another effect characteristic of reaction-diffusion waves, [6] and [21]. The value of injected current chosen is also within the type I intermittency region. After the collision at the boundaries, all the spikes disappear and the axon stays in a non uniform and

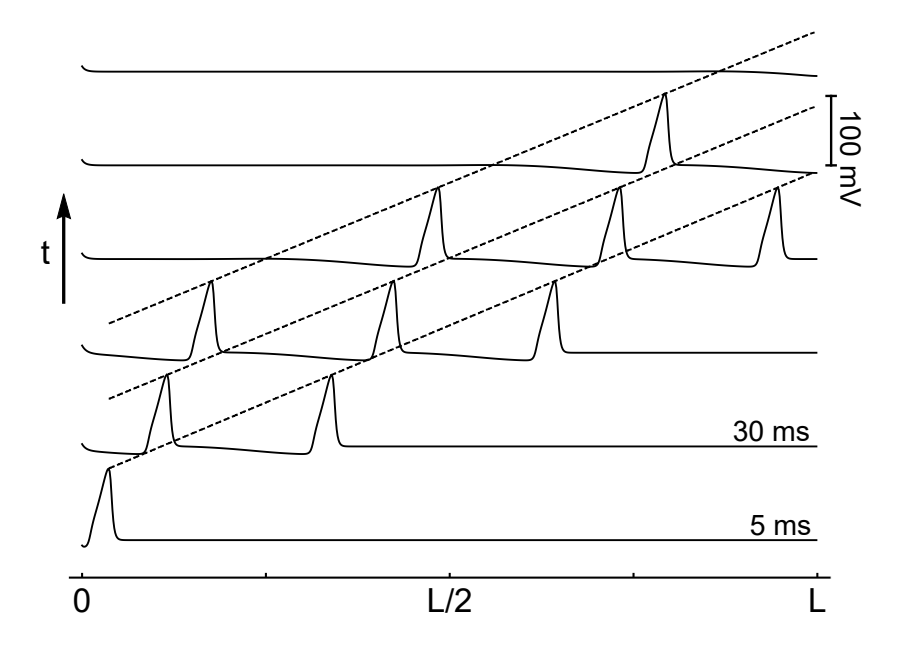


Figure 3: Snapshots of the solutions -V(x,t) of (4)-(5). The conditions are the same as in figure 2, except that the injected current at x = 0 is $i_0 = 57.7 \,\mu\text{A/cm}^2$, during the entire simulation. The system is in the type I intermittency region, generating a total of three spikes. The dotted lines are three characteristic curves of the solutions of the HH equations. The speed of the front action potential spike is the same as in figure 2. During this observation time, the characteristic curves appear to be approximately parallel. Action potential signals annihilate at the boundary x = L.

non excitable state, with no more spikes being generated at the injection points.

Through the results illustrated in figures 2, 3, and 4, we have shown that the solutions of the HH equations do not propagate as elastic waves, as conjectured by Hodgkin and Huxley, but behave instead as reaction diffusion waves. In all three cases analysed, we have shown that the action potentials are never reflected at the axon boundary. Furthermore, the behaviour seen in figure 4 is also not compatible with that of elastic waves, where the amplitudes would be halved when the action potential splits in two and the collision of two waves would not result in annihilation.

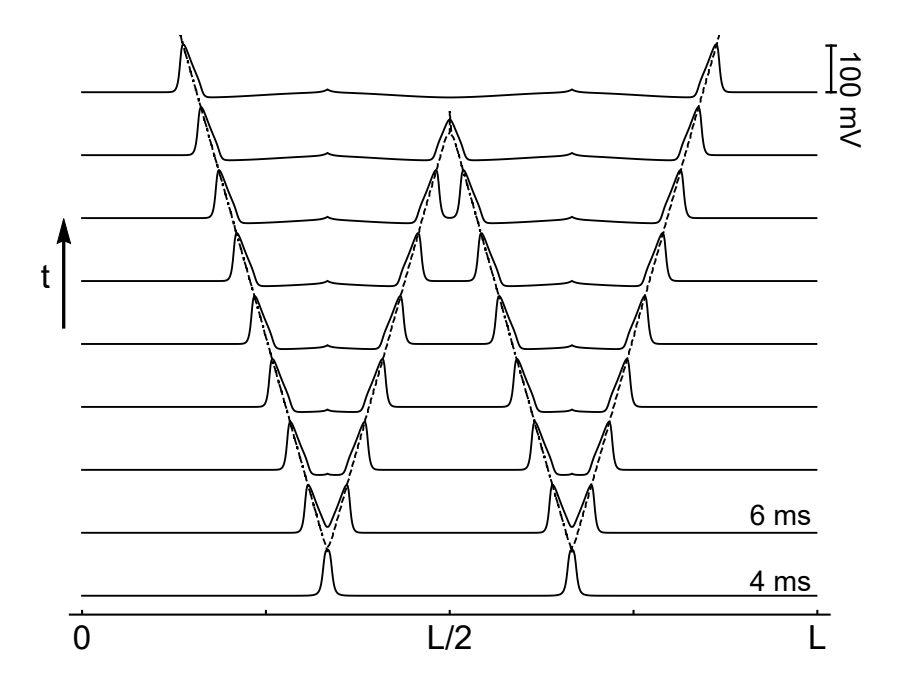


Figure 4: Snapshots of the solutions -V(x,t) of (4)-(5), for two injected currents at axon positions x = L/3 and x = 2L/3. The injected currents have a value of 57.0 μ A/cm², during the entire simulation. The characteristic curves are represented by the dotted lines.

3.3 Action potential waves

In order to better perceive how the action potential changes as it propagates along the axon, in this section we have extended the spatial domain of the simulation to L = 250 cm, discretized in M = 2000 small intervals. In figure 5, the axon is excited at x = 0 with a large current i_0 , in three different oscillatory regions of figure 1. In subfigures a), we show the same diagram seen in figures 2 to 4. In b), we show the speed with which the first 40 action potentials propagate at the beginning of the axon (x << L) – we called this initial velocity speed₀, and the n^{th} action potential to be generated by the system is identified by the horizontal axis N. In subfigures c), we show how the speed of the action potentials evolves as they propagate along the axon – the dashed lines represent the first 29 action potentials, and the full lines represent action potentials 30 to 40. So, we are able to distinguish the transient behaviour of the first spikes from that of the later spikes, which correspond to an asymptotic state of the system.

In figures 5.1, we excited the neurone with current $i_0 = 200 \ \mu\text{A/cm}^2$, in the periodic oscillatory region (see figure 1). The initial velocity of the action po-

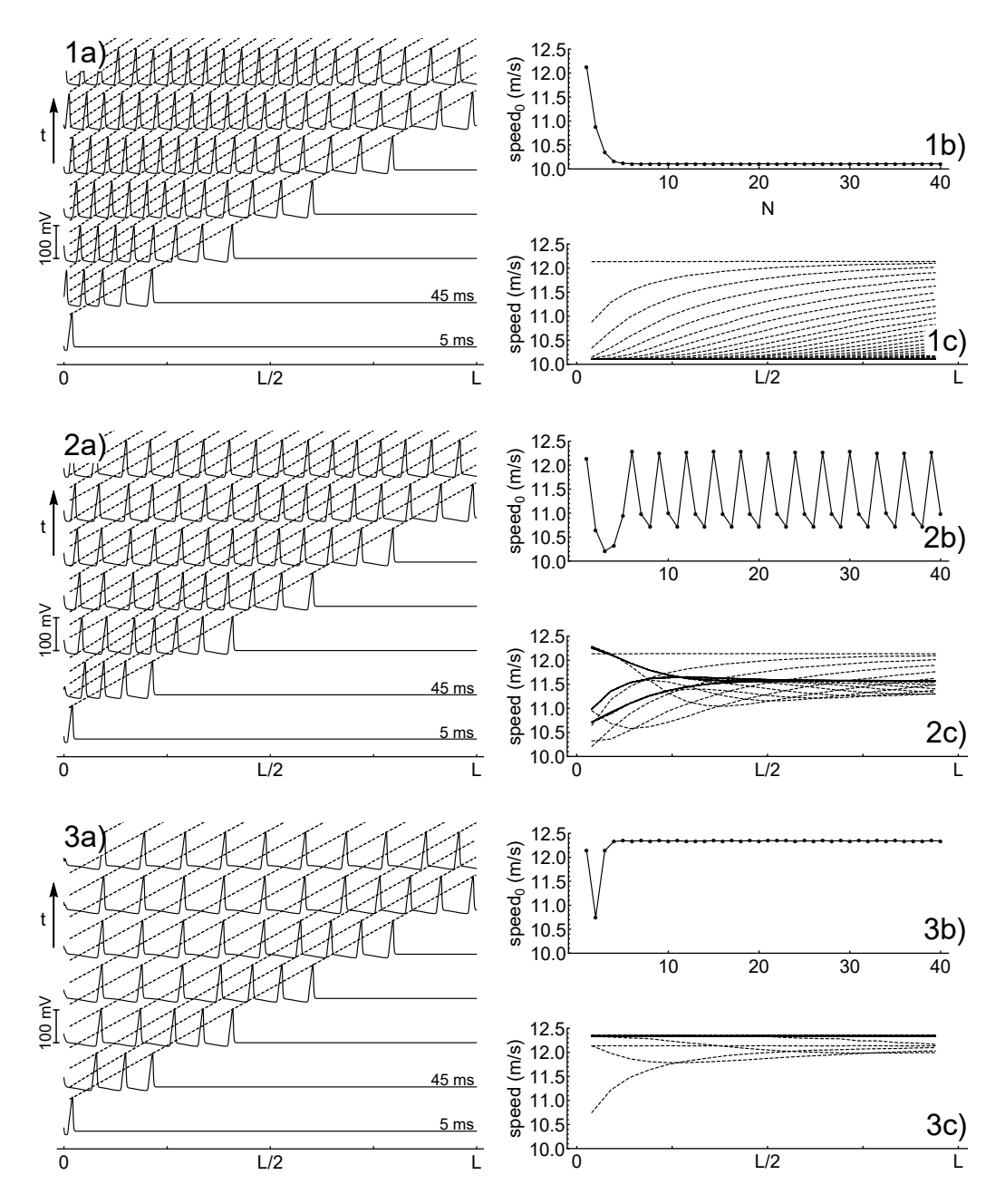


Figure 5: a) Snapshots of the solutions -V(x,t) of (4)-(5), for injected currents 1) $i_0 = 200.0 \ \mu\text{A/cm}^2$, 2) $i_0 = 300.0 \ \mu\text{A/cm}^2$, and 3) $i_0 = 351.4 \ \mu\text{A/cm}^2$, at x = 0 during the entire simulation. We also show some of the characteristic curves of the solutions. b) Initial velocity (for x << L) of the first 40 action potentials generated by the system. c) Evolution of the speed of the first 40 action potentials as they propagate throughout the axon – dashed lines correspond to spikes 1 to 29, and full lines to spikes 30 to 40. In 1) and 3), we have an asymptotically oscillatory response, and, in 2), a chaotic response.

tentials converges quickly to a fixed value, as seen through speed₀. While this initial velocity converges, the action potentials still accelerate while propagating through the axon. Eventually, all of the action potentials attain the same initial velocity and final velocity, propagating with constant speed.

In figures 5.2, the neurone was excited with current $i_0 = 300 \,\mu\text{A/cm}^2$, in the chaotic oscillatory region $[I_2^*, I_3^*]$. The initial velocity of the action potentials converges to a period-3 solution. However, as the spikes propagate along the axon, this period-3 disappears, giving way to a constant propagation speed. The apparently chaotic effect of this region in the propagation speeds of the action potentials is merely transient, dissipating as the spikes advance through the axon.

In figures 5.3, the chosen current was $i_0 = 351.4 \,\mu\text{A/cm}^2$, in the small chaotic oscillatory region $[I_4^*, I_5^*]$. Even though this small region shows very clear period bifurcations which give way to a chaotic intermittency regime (as shown in [4]), the velocity profiles do not give any hint of this. As seen in the figure, the initial velocity quickly converges to a fixed value, which is maintained as the action potentials travel along the axon. The chaoticity of signals is present, not in the velocity of propagation, but in the non uniformity of the distances between consecutive action potential spikes.

In figure 6, we show the velocity profiles for different values of current i_0 for the whole oscillatory region $[I_1^*, I_5^*]$.

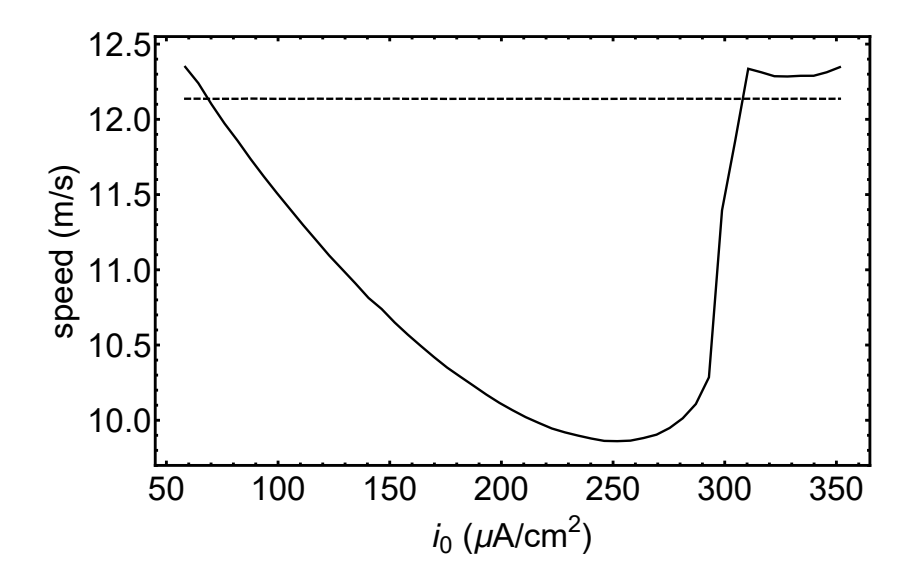


Figure 6: Action potential propagation speeds for the entire oscillatory region $[I_1^*, I_5^*]$. The dashed line represents the speed of the first action potential, which is always constant. The full line represents the final speed of the later action potential spikes (N > 30), measured at the end of the axon, as in figures 5c).

It can be seen that the speed of the first action potential spike is the same (v = 12.14 m/s), regardless of the value of injected current. We had already observed the same value for the type I intermittency region in figures 2 and 3. On the other hand, the final speed varies as the injected current increases. At first the velocity decreases, reaching its lowest value around 250 μ A/cm². Then, it increases until I_2^* , where a transient chaos influences the period and velocity with which the spikes are generated (as shown in figure 5.2). In $[I_3^*, I_4^*]$, the final velocity of the system stabilises, only varying slightly as the current keeps increasing, until it stops existing at the end of the oscillatory region.

In figure 7, we have measured the velocities of the action potentials in the type I intermittency region, and we have analysed how their profile changes as the transition to the oscillatory region occurs.

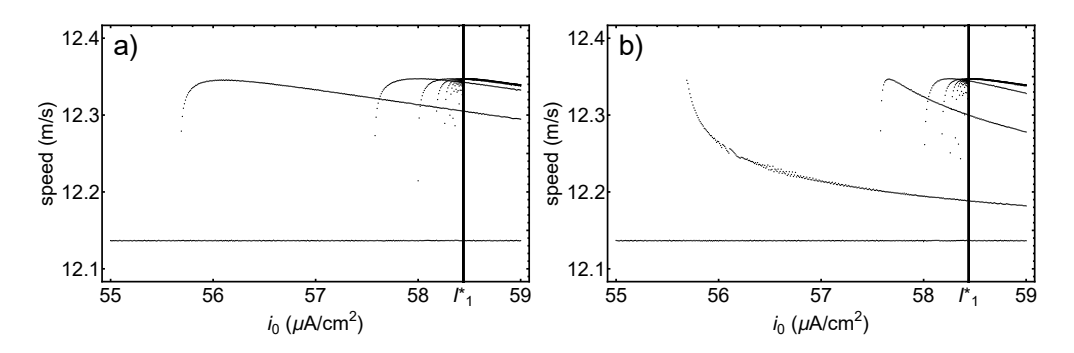


Figure 7: Propagation speeds of action potential spikes in the vicinity of I_1^* . The horizontal line corresponds to the velocity of the first spike, which remains constant throughout the axon (see figure 5). In a), the speed of the action potentials is measured at the beginning of the axon; in b), it is measured at the end of the axon. All of the dots correspond to the measured velocities of the action potentials. The transition from type I intermittency to periodic oscillations occurs at the vertical line I_1^* . The top thick line for $i_0 > I_1^*$ is the full line seen in figure 6.

For low values of current ($i_0 < 55.5 \,\mu\text{A/cm}^2$), only one action potential speed can be seen — the horizontal line around v = 12.14 m/s. This is the speed of the first action potential, which is the only one that is produced for these values of current (shown in figure 2, where $i_0 = 55.0 \,\mu\text{A/cm}^2$). Once again, the speed of the first action potential always has the same value and remains constant during propagation, both in the intermittency and oscillatory regions. This is consistent with what we have seen in figures 2, 3, 5, and 6. As the current increases ($55.5 < i_0 < I_1^*$), we can see additional action potential spike speeds. At $i_0 = 57.7 \,\mu\text{A/cm}^2$, we can distinguish three different propagation speeds, corresponding to the three action potentials seen in figure 3, where the same current was injected. Whereas

in figure 3 all of the characteristic curves seemed to be linear, here we can clearly see that the speed of the second and third spikes do not remain constant during the propagation, having different values at the beginning (figure 7a) and end (figure 7b) of the axon. As the current approaches I_1^* , we see how the number of spikes increases exponentially (an effect of type I intermittency, [4]), and the velocity profile leads into the profile seen in the oscillatory region.

In figure 8, we have calculated the asymptotic dispersion relation for the oscillatory region $[I_1^*, I_4^*]$. In a), we have calculated the period and wavelength between spikes 30 and 31, at the last quarter of the axon (as shown in figure 5, in this region, all the action potentials have attained their stable final velocity). In b) we have calculated the dispersion relation at the same location in the axon, but between spikes 1 and 2, before the system has reached the asymptotic regime. This shows that the asymptotic dispersion relation of the oscillatory regime of the HH equation 1 is not linear.

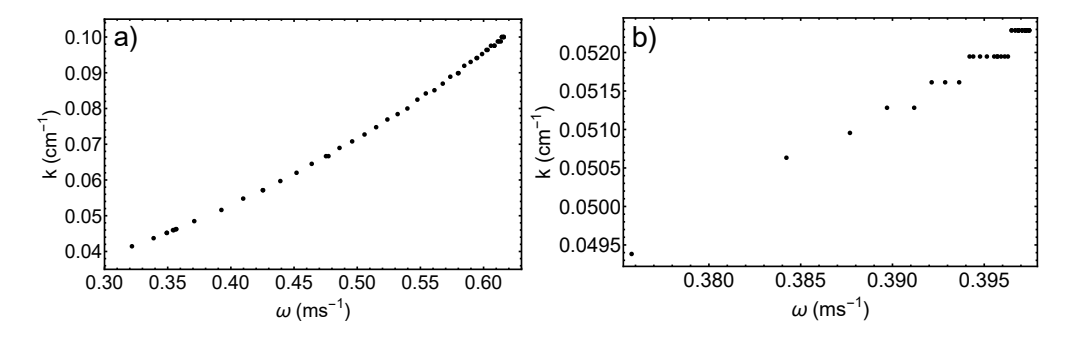


Figure 8: Asymptotic dispersion relation for the oscillatory region $[I_1^*, I_4^*]$. The measurements were made in the last quarter of the axon. In a), the period and wavelength ($\lambda = 2\pi/k$) were calculated through spikes 30 and 31. For reference, in b), spikes 1 and 2 were used.

4 Final remarks and conclusions

To test the predictions of the HH model (1) with patch clamp data and without the assumptions (2) and (3), the first requirement is to measure the current as a function of the spatial position along the axon. Due to the diffusive nature of the current propagation along the axon, the second requirement is to test if action potentials spikes propagate without attenuation along the axon. Without the fulfillment of these requirements, the HH model can not be validated.

Other important predictions of the HH model (1) about the propagation of axonal signals is the existence of a saddle-node bifurcation of limit cycles and the

existence of the type I intermittency phenomenon. This bifurcation is tuned by the magnitude of the applied current i_0 to the axon. Let I_1^* be the i_0 bifurcation value.

For $i_0 < I_1^*$, and depending on the electrophysiological state of the axon (transmembrane potential, ionic concentrations, etc.), we may have no spikes at all, one spike or several spike responses up to some maximum number N. This number N relates with I_1^* and i_0 through the relation $\ln N = C - (\ln(I_1^* - i_0))/2$, characteristic of type I intermittency, [4]. As far as we know, this multi-spike phenomenon has never been reported in a voltage clamp experiment. On the other hand, its observation would corroborate the existence of the bifurcation predicted by the HH model. If this behaviour is not observed, it can happen that the validity of the HH model would be for values of i_0 much below I_1^* . In this case, the only steady state is the equilibrium associated to the Nernst potentials and, due to the non-linear nature of action potential signals, the existence of a travelling spiky signal would be difficult to justify in the framework of the HH model.

The importance of the existence of a saddle-node bifurcation of limit cycles implies that axonal signals may respond to external stimulus with an approximately periodic, or even chaotic response. The observation of this type of response would be an important biological mechanism predicted by the HH model.

Even in the case of negative observations of the several spiky phenomenon and associated intermittency, it would be important to observe the possibility of propagation of signals in the two opposite directions of the axon, a phenomenon that is believed to occur, [17], as well as the action potential dynamics when two isolated action potential spikes collide. These are intrinsic phenomena associated with the diffusive nature of the HH model and of reaction-diffusion systems of equations. If these interaction patterns fail, then we can not say that action potentials are reaction-diffusion waves. In this case, the problem of the derivation of a more detailed model for the study of electric phenomena in cells and axons should be reconsidered, [5].

Acknowledgements

RD would like to thank IHÉS for hospitality and Simons Foundation for support.

References

- [1] Aslanidi, O. V. and Mornev, O. A., Can colliding nerve pulses be reflected?, ETP Lett., 65(7) (1997) 579-585.
- [2] Appali, R., van Rienen, U. and Heimburg, T., A comparison of the Hodgkin-Huxley model and the soliton theory for the action potential in nerves, *in*

- Advances in Planar Lipid Bilayers and Liposomes, Iglic, A. (ed), vol 16 (2012) 275-299. Doi: 10.1016/B978-0-12-396534-9.00009-X
- [3] Bezanilla, F., Gating currents, J. Gen. Physiol. 150(7) (2018) 911-932, doi: 10.1085/jgp.201812090.
- [4] Cano, G. and Dilão, R., Intermittency in the Hodgkin-Huxley model, Journal of Computational Neuroscience, 43 (2017) 115-125, doi: 10.1007/s10827-017-0653-9, 2017.
- [5] Dilão, R., An electrophysiology model for cells and tissues, IHES preprint, http://preprints.ihes.fr/2019/P/P-19-09.pdf, 2019.
- [6] Dilão, R. and Volford, A., Excitability in a model with a saddle-node homoclinic bifurcation, Discrete and Continuous Dynamical Systems series B, 4 (2004) 419-434.
- [7] Dilão, R. and Sainhas, J., Validation and calibration of models for reaction-diffusion systems, International Journal of Bifurcation and Chaos, 8 (1998) 1163-1182.
- [8] Ermentrout, G. B. and Terman, D., Mathematical Foundations of Neuroscience, Springer, New York, 2010.
- [9] Hodgkin, A. L., Huxley, A. F., A quantitative description of membrane current and its application to conduction and excitation in nerve, J. Physiol. 117 (1952) 500–544.
- [10] Hill, B., Ionic Channels of Excitable Membranes, 2nd edition, Sinauer, Sunderland, 1992.
- [11] Hoppensteadt, F. C. and Peskin, C. S., Modeling and Simulations in Medicine and the Life Sciences, Springer, New York, 2002.
- [12] Hassard, B., Bifurcation of periodic solutions of the Hodgkin-Huxley model for the squid giant axon, J. Theor. Biol. 71 (1978) 401-420.
- [13] Keener, J. and Sneyd, J., Mathematical Physiology, Springer, New York, 1998.
- [14] Leuchtag, H. R., Voltage-sensitive ion channels, biophysics of molecular excitability, Springer, The Netherlands, 2008.
- [15] Leuchtag, H. R., What's wrong with the Hodgkin-Huxley model? An Exercise in Critical Thinking, Biophysical J. 112(3), supp. 1, 464A (2017), DOI: 10.1016/j.bpj.2016.11.2488.

- [16] Meunier, C. and Segev, I., Playing the devil's advocate: is the Hodgkin-Huxley model useful?, TRENDS in Neurosciences 25(11) (2002) 558-563.
- [17] Oh, S. H., Clinical electromyography. Nerve conduction studies, Lippincott Williams & Wilkins, Philadelphia, 2003.
- [18] Purves, D., Augustine, G. J., Fitzpatrick, D., Hall, W. C., Lamantia, A.-S., McNamara, J. O., Williams, S. M., Neuroscience, Sinauer Associates, Inc., 3rd Edition, 2004.
- [19] Phillips, R., Kondev, J., Theriot, J. and Garcia, H., Physical Biology of the Cell (2nd Edition), Garland Science, 2012.
- [20] Rinzel, J. and Miller, R. N., Numerical calculation of ctable and unstable periodic solutions to the Hodgkin-Huxley equations, Mathematical Biosciences 49 (1980) 27–59.
- [21] Sainhas, J., and Dilão, R., Wave optics in reaction-diffusion systems, Phys. Rev. Lett., 80 (1998) 5216-5219.
- [22] Tasaki, I., Physiology and Electrochemistry of Nerve Fibers, Academic Press, 1982.
- [23] Zabusky, N. J. and Kruskal, M. D., Interaction of "solitons" in a collisionless plasma and the recurrence of initial states, Phys. Rev. Lett **15**(6) (1965) 240-243.